

Non-Abelian braid statistics as a holonomy in an exactly solvable lattice model

Ville Lahtinen and Jiannis K. Pachos

School of Physics & Astronomy, University of Leeds, Leeds LS2 9JT, UK

(Dated: December 5, 2019)

Kitaev's honeycomb lattice model is an exactly solvable model, where the vortices are conjectured to be non-Abelian Ising anyons. By employing the Majorana fermionization technique and exact diagonalization, we solve this model on a torus for arbitrary vortex configurations. This enables the evaluation of the non-Abelian holonomy associated with the adiabatic braiding of two vortices. We identify ranges in the parameters of the model where the holonomy coincides with the statistics of Ising anyons. Finally, we present an explicit scheme for the vortex creation, transport and characterization.

A striking feature of topological phases of matter is that they can support anyons. These are quasiparticles whose adiabatic exchange causes non-trivial evolution in the state of the system. If the evolution is given by a phase factor, the anyons are called Abelian. The presence of non-Abelian anyons gives rise to spectral degeneracy and their braiding is described by a unitary matrix acting on the degenerate states. Demonstrating the anyonic statistics conclusively characterizes the topological phase of the system. The realization of such phases is essential for topological quantum computation [1], where the statistics is employed for error-free quantum information processing.

The best known many-body system conjectured to support non-Abelian statistics is the fractional quantum Hall liquid [2]. Other proposals include the p -wave superconductor [3] as well as various lattice models [4, 5, 6, 7]. These systems are either tailored to identically support non-Abelian statistics and have complex physical realizations, or they can be described by simple Hamiltonians, but their statistical behavior is merely conjectured. In particular, for the fractional quantum Hall states the arguments rely on properties of trial wave functions derived from conformal field theories [8, 9, 10], whereas for the lattice models explicit calculations have not been attempted.

In this letter we present an explicit demonstration of non-Abelian statistics using Kitaev's honeycomb lattice model [6]. This is performed by employing the Berry phase technique [8] to calculate the non-Abelian holonomy associated with the adiabatic braiding of anyons. By using exact eigenstates of a finite size system, we obtain a unitary matrix that corresponds to the statistics of the conjectured Ising anyons to the accuracy of 10^{-2} . Together with the non-Abelian fusion rules of these anyons [11, 12], this conclusively demonstrates the non-Abelian character of Kitaev's model. Further, we present a scheme for creating, transporting and characterizing anyons that could be used in the proposed physical implementations [13].

Kitaev's model [6] is comprised of spin-1/2 particles residing on the vertices of a honeycomb lattice. The spins

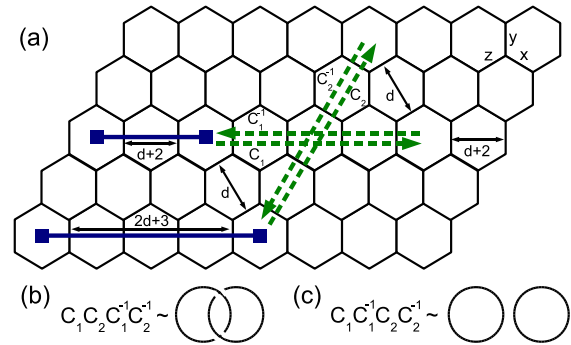


FIG. 1: (a) A unit cell of the honeycomb lattice containing two vortex pairs. This vortex configuration is created by setting $u_{ij} = -1$ on the links crossed by solid lines and $u_{ij} = 1$ on all other links. The parameter d controls the minimal vortex separation. It is related to the cell dimensions through $M = 2(2d + 4)$ and $N = 2d + 3$ (picture not on scale). The four dashed arrows C_1 , C_1^{-1} , C_2 and C_2^{-1} are the oriented parts of the path C along which the vortices are moved. (b) $C_l = C_1 C_2 C_1^{-1} C_2^{-1}$ is topologically equivalent to a link. (c) $C_o = C_1 C_1^{-1} C_2 C_2^{-1}$ is topologically equivalent to two unlinked loops.

interact according to the Hamiltonian

$$H = - \sum_{(i,j)} J_{ij} \sigma_i^\alpha \sigma_j^\alpha - \sum_{(i,j,k)} K_{ijk} \sigma_i^x \sigma_j^y \sigma_k^z, \quad (1)$$

where $J_{ij} = (J_\alpha)_{ij}$ are positive couplings and α is either x , y or z when (i, j) is an x , y or z -link, respectively (see Fig. 1(a)). The second term is an effective magnetic field with positive couplings K_{ijk} , where the sum runs over next to nearest neighbor triplets as described in [11]. The Hamiltonian has the symmetry $[H, \hat{w}_p] = 0$, where $\hat{w}_p = \sigma_1^x \sigma_2^y \sigma_3^z \sigma_4^x \sigma_5^y \sigma_6^z$ (enumeration clockwise around the plaquette starting from lower right corner) are plaquette operators whose eigenvalues $w_p = -1$ are interpreted as having a *vortex* on plaquette p . The Hamiltonian can be diagonalized by representing the spin operators as $\sigma_i^\alpha = i b_i^\alpha c_i$, where c_i, b_i^x, b_i^y and b_i^z are Majorana fermions. Subsequently, the Hamiltonian takes the form $H = \frac{i}{4} \sum_{i,j} \hat{A}_{ij} c_i c_j$, where

$$\hat{A}_{ij} = 2J_{ij} \hat{u}_{ij} + 2 \sum_k K_{ijk} \hat{u}_{ik} \hat{u}_{jk}, \quad \hat{u}_{ij} = i b_i^\alpha b_j^\alpha. \quad (2)$$

The eigenstates of the original Hamiltonian (1) are subject to the constraint

$$D_i |\Psi\rangle = |\Psi\rangle, \quad D = b_i^x b_i^y b_i^z c_i, \quad [D_i, \sigma_j^\alpha] = 0. \quad (3)$$

Since $[H, \hat{u}_{ij}] = 0$, the Hilbert space splits into sectors each labelled by u , a certain pattern of eigenvalues u_{ij} . The configurations u can be understood as a classical Z_2 gauge field with local gauge transformation operators D_i . The plaquette operators $\hat{w}_p = \prod_{(i,j) \in p} \hat{u}_{ij}$ can be identified with gauge invariant Wilson loop operators. Fixing the gauge field configuration u gives a particular vortex configuration.

Define a partition of the lattice into unit cells of $2MN$ spins and assume u to be fixed in each cell such that it creates the four vortex configuration shown in Fig. 1(a). Then the Hamiltonian can be diagonalized by employing Fourier transformation. This gives the double spectrum

$$H = \int d^2\mathbf{p} \sum_{i=1}^{MN} \frac{\epsilon_{i,\mathbf{p}}}{2} \left[b_{i,\mathbf{p}}^\dagger b_{i,\mathbf{p}} - b_{i,-\mathbf{p}} b_{i,-\mathbf{p}}^\dagger \right], \quad (4)$$

where the integration is restricted to the first Brillouin zone, $b_{i,\mathbf{p}}$ are fermionic operators satisfying $\{b_{i,\mathbf{p}}^\dagger, b_{j,\mathbf{p}'}\} = \delta_{ij} \delta_{\mathbf{p},\mathbf{p}'}$ and $\pm \epsilon_{i,\mathbf{p}}$ are the corresponding eigenvalues. The explicit expression for the Fourier transform of A for an arbitrary unit cell is derived in [11]. There it was shown that when the unit cell contains $2n$ well separated vortices and the system is in the non-Abelian phase ($J_x = J_y = J_z = 1$, $K > 0$), the low energy spectrum comprises of n zero modes ($\epsilon_{i,\mathbf{p}} \approx 0$, for $i = 1, \dots, n$ and all \mathbf{p}) separated from the rest of the fermionic spectrum by a finite energy gap. In our case of four vortices this implies fourfold ground state degeneracy arising from a pair of zero modes that can be either occupied or empty

$$|\Psi_{i_1 i_2}\rangle = (b_1^\dagger)^{i_1} (b_2^\dagger)^{i_2} |\text{gs}\rangle, \quad (5)$$

where $i_1, i_2 = 0, 1$ and $|\text{gs}\rangle = \prod_{\mathbf{p}} \prod_{i=1}^{MN} b_i(\mathbf{p}) |\phi\rangle$ is the ground state. For convenience we choose the reference state such that $b_{i,\mathbf{p}}^\dagger |\phi\rangle = 0$.

To simplify the calculations we restrict the system to be defined on a torus of size $2MN$. This corresponds to taking only the $\mathbf{p} = 0$ term of (4). Numerical diagonalization of A , (see (2)), gives $2MN$ eigenvectors ψ_i^\pm satisfying the double spectrum $A\psi_i^\pm = \pm \epsilon_i \psi_i^\pm$, where ϵ_i coincide with the eigenvalues of the diagonalized Hamiltonian (4). We construct a representation of the two degenerate ground states $|\Psi_{10}\rangle$ and $|\Psi_{01}\rangle$ as

$$|\Psi_i\rangle = \sum_{\substack{\{k,\dots,l=1\} \\ k,\dots,l \neq i}}^{MN-1} \frac{\varepsilon_{k,\dots,l}}{\sqrt{(MN-1)!}} \psi_k^- \otimes \dots \otimes \psi_l^-, \quad (6)$$

where $i = 1, 2$, respectively, and $\varepsilon_{k,\dots,l}$ is the fully anti-symmetric tensor of rank $MN-1$. In general, such states are too large to be stored in a computer, because their

number of elements grows exponentially with the system size. However, the inner product of two such vectors, each depending possibly on some parameters t and t' , can be efficiently calculated and is given by

$$\langle \Psi_i(t) | \Psi_j(t') \rangle = \det(B_{ij}^{tt'}), \quad (7)$$

where $[B_{ij}^{tt'}]_{kl} = \psi_k^{-\dagger}(t) \psi_l^-(t')$.

It has been conjectured by conformal field theory arguments that this system supports the Ising anyon model [6]. This model has three types of particles: 1 (vacuum), ψ (fermion) and σ (non-Abelian anyon). In [11] these are identified with the ground state, the fermion modes $b_{\mathbf{p}}^\dagger$ and the vortices of Kitaev's model, respectively. The non-trivial fusion rules are given by $\psi \times \psi = 1$, $\psi \times \sigma = \sigma$ and $\sigma \times \sigma = 1 + \psi$. The last fusion rule implies that there is a degree of freedom associated with the different ways a number of σ 's can fuse when their total anyonic charge is fixed. Taking the four σ particles to fuse to a ψ , this fusion degree of freedom is encoded in the two dimensional *fusion space*, $V_{\sigma^4}^\psi$. Its basis can be chosen to be the states associated with the two distinct pair-wise fusion channels:

$$\begin{aligned} (\sigma \times \sigma) \times (\sigma \times \sigma) &\rightarrow \psi \times 1 = \psi, \\ (\sigma \times \sigma) \times (\sigma \times \sigma) &\rightarrow 1 \times \psi = \psi. \end{aligned} \quad (8)$$

In [11] the number of intermediate ψ 's is identified with the number of occupied zero modes. Hence, a suitable basis is given by the states $\{|\Psi_1\rangle, |\Psi_2\rangle\}$ (see (6)). The braid operator, R , describes the statistics of the σ anyons. In particular, the *monodromy* operator, R^2 , corresponds to one particle encircling another clockwise. On the basis (8) the monodromy of two σ 's that belong to different pairs is given by

$$R^2 = e^{-\frac{\pi}{4}i} \begin{pmatrix} 0 & 1 \\ 1 & 0 \end{pmatrix}. \quad (9)$$

We demonstrate this statistical property of the σ anyons by adiabatically transporting a vortex around another. The evolution in $V_{\sigma^4}^\psi$ is given by evaluating the corresponding holonomy [14]. Consider a Hamiltonian $H(\lambda)$ with n -fold degeneracy $\{|\Psi_i(\lambda)\rangle | i = 1, \dots, n\}$ that depends on some parameters λ . When we adiabatically vary λ along a closed path C , the evolution of the degenerate subspace is given by the holonomy $\Gamma_C = P \exp \oint_C A^\mu(\lambda) d\lambda_\mu$, where $[A^\mu(\lambda)]_{ij} = \langle \Psi_i(\lambda) | \frac{d}{d\lambda^\mu} | \Psi_j(\lambda) \rangle$ and P denotes path ordering in λ . To simulate the vortex transport, we discretize the path C into T infinitesimal intervals of length $\delta\lambda$ with $\lambda(t)$ denoting the control parameter value at step t . It follows that the holonomy takes the form

$$\Gamma_C = P \prod_{t=1}^T \left(\sum_{i=1}^n |\Psi_i(\lambda(t))\rangle \langle \Psi_i(\lambda(t))| \right), \quad (10)$$

i.e. it is given by the ordered product of projectors onto the ground state space at each step t .

For convenience we choose C such that it is a loop in both the space of four vortex and gauge field configurations [15]. This is illustrated in Fig. 1(a), where the path C (dashed lines) is split into four parts. Different ordering of these parts corresponds to the topologically inequivalent paths C_l and C_o given in Fig. 1(b) and (c), respectively. Neither path spans any area and hence all contribution to the holonomy is topological. Since u is a static background field, we need to introduce classical control parameters to physically implement the transport. Assuming local control of J and K on all links, we see from (2) that the simultaneous sign change of J and K on link (i, j) is equivalent to changing $u_{ij} \rightarrow -u_{ij}$. This either generates a vortex pair or transports a vortex through the link (i, j) . In our simulation this is performed in S infinitesimal steps. Taking $\lambda = (J, K)$, the discrete holonomy (10) for the degenerate states (6) becomes

$$\Gamma_C = P \prod_{t=1}^T \begin{pmatrix} \det(B_{11}^{t,t+1}) & \det(B_{12}^{t,t+1}) \\ \det(B_{21}^{t,t+1}) & \det(B_{22}^{t,t+1}) \end{pmatrix}, \quad (11)$$

where we have used the inner product (7). Therefore, the holonomy can be evaluated by diagonalizing the Hamiltonian at each step t and multiplying together the inner products of the eigenstates from successive steps according to (11). We perform this for the three parametrizations shown in Table I.

	d	S	T	$2MN$
(i)	1	$2 \cdot 10^3$	$32 \cdot 10^3$	120
(ii)	2	$2 \cdot 10^3$	$48 \cdot 10^3$	224
(iii)	3	$4 \cdot 10^3$	$128 \cdot 10^3$	360

TABLE I: Three parametrizations (i), (ii) and (iii) for which the holonomy is evaluated. Here $T = 8S(d+1)$ and the number of spins is $2MN = 8(d+2)(2d+3)$. S has been increased in (iii) to suppress accumulation of discretization errors due to longer path.

Since the spectrum varies slightly with t during the braiding process, we define the minimal fermion gap, Δ , and the maximum energy splitting between the two ground states, δ , by

$$\Delta = \min_t (\epsilon_3^t - \epsilon_2^t), \quad \delta = \max_t (\epsilon_2^t - \epsilon_1^t), \quad (12)$$

respectively, where ϵ_i^t is the i th eigenvalue at step t . These are plotted in Fig. 2, where we observe that both the fermion gap and the level of degeneracy improve as K and d increase. Under the adiabatic approximation the holonomy corresponds to the exact time evolution when $\Delta \gg \delta$ and $\delta \rightarrow 0$. To physically accommodate these conditions in a finite size system, the vortex transport should be fast enough compared to δ for the states

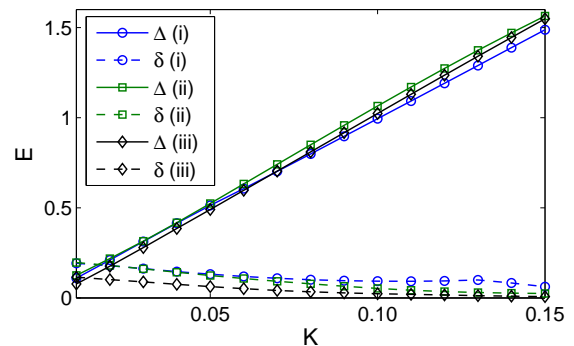


FIG. 2: The minimal fermion gap Δ (solid lines) and the maximum energy splitting between the ground states δ , (12) (dashed lines) as functions of K for parametrizations (i) (circles), (ii) (squares) and (iii) (diamonds) given in Table I. The fermion gap grows linearly and the degeneracy improves with increasing K for all parametrizations. The fermion gap is relatively insensitive to the vortex separation, whereas the degeneracy improves when the vortices are further apart.

$|\Psi_i\rangle$, $i = 1, 2$ to appear as degenerate, but slow enough compared to Δ so that no fermionic excitation is produced. We see from Fig. 2 that $\frac{\delta}{\Delta} \lesssim 10^{-2}$ for (iii) when $K \gtrsim 0.07$. This region can support the adiabaticity conditions and hence we take $K \approx 0.07$ as a lower bound for identifying a stable topological phase.

To quantitatively study the holonomy, we introduce a fidelity measure for a target matrix U and a test matrix V as

$$s(U, V) = \frac{1}{4} \text{tr} (UV^\dagger + VU^\dagger). \quad (13)$$

For U, V unitary 2×2 matrices we have that $s(U, V) = 1$ if and only if $U = V$, while in general $s(U, V) \leq 1$. Let Γ_{C_l} be the numerically obtained holonomy with off-diagonal elements $re^{i\theta}$, $0 \leq r \leq 1$. After fixing the gauge [16], we evaluate the unitarity measure, $s(\mathbb{1}, \Gamma_{C_l} \Gamma_{C_l}^\dagger)$, Fig. 3(a), and the two different fidelity measures of the holonomy: $s(|R^2\rangle, |\Gamma_{C_l}\rangle) = r$ (measure of off-diagonality that characterizes R^2) and $\bar{s}(R^2, \Gamma_{C_l}) = \frac{1}{2}[s(R^2, \Gamma_{C_l}) + 1] = \frac{1}{2}[r \cos(\frac{\pi}{4} + \theta) + 1]$ (the total fidelity), Fig. 3(b-d) [17].

First, we observe that the unitarity measure is above 98% for all parametrizations when $K \lesssim 0.10$, which we take as an upper bound for identifying a stable topological phase. For (i) we obtain no significant off-diagonality due to the small size of the system. However, for (ii) the holonomy is predominantly off-diagonal (e.g. $r > 0.9$) for $0.02 \lesssim K \lesssim 0.04$, and for (iii) for $0.02 \lesssim K \lesssim 0.09$. The total fidelity, \bar{s} , accounts also for the overall phase and can distinguish between the Ising ($\bar{s} = 1$) and $SU(2)_2$ ($\bar{s} = \frac{1}{2}$) anyon models whose monodromies only differ by an overall phase factor, $e^{-i\pi/2}$. We observe that for (ii) there is a small region around $K \approx 0.02$ and for (iii) there is a wider region, $0.08 \lesssim K \lesssim 0.10$, where $\bar{s} > 0.9$. The maximum fidelities are given by 0.981 and

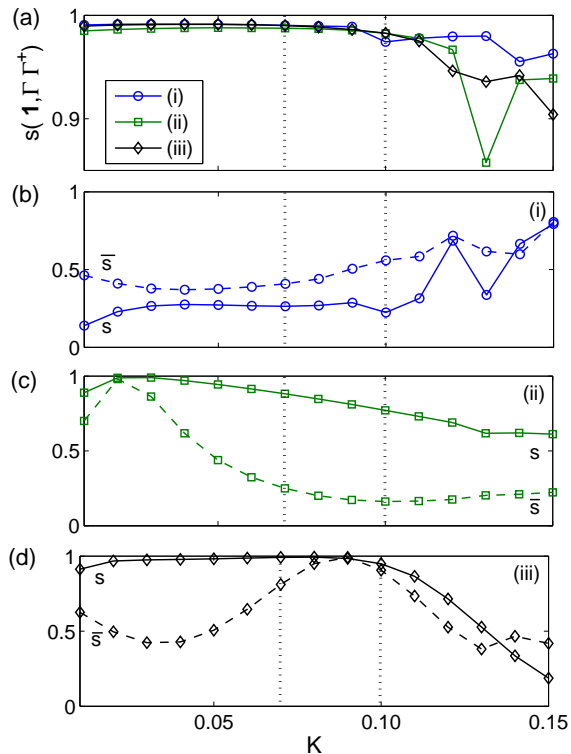


FIG. 3: (a) The unitarity measure, $s(\mathbb{1}, \Gamma_{C_l}^\dagger \Gamma_{C_l})$, as a function of K for the three configurations given in Table I. The measure of off-diagonality, $s(|R^2|, |\Gamma_{C_l}|)$ (solid line), and the total fidelity, $\bar{s}(R^2, \Gamma_{C_l})$ (dashed line), as a function of K for the parametrizations (b) (i) (circles), (c) (ii) (squares) and (d) (iii) (diamonds). Based on unitarity and the energy gap behavior, we expect a stable phase in the area $0.07 \lesssim K \lesssim 0.10$ bounded by the dashed vertical lines.

0.991, respectively. Parametrization (iii) also has a region $0.02 \lesssim K \lesssim 0.05$ where $\bar{s} \approx \frac{1}{2}$ with error $\pm 10^{-1}$. However, we disregard this regime, because such a region does not exist for the smaller system (ii) and it lies outside the domain which we consider as a stable phase. Further, we check for all parametrizations and all K that $\Gamma_{C_o} \approx \mathbb{1}$ with error less than 10^{-2} , that for $K = 0$ the holonomy vanishes and that $\Gamma_{C_l^{-1}} = \Gamma_{C_l}^\dagger$ when the direction of braiding is reversed. Hence, we are able to identify finite regions of K where the adiabaticity conditions hold and the non-Abelian statistics corresponds to the Ising anyon model for sufficiently large system sizes and for a variety of paths.

Finally, our method of locally changing the couplings J and K translates directly to how one could physically implement the creation and transport of anyons. As the energy of the system is known to depend on the zero mode populations [11], the effect of braiding is also detectable through spectral means. Since the monodromy results in swapping these populations between the vortex pairs, the energy behavior of the system will be different when the vortices from a single pair are brought close together before and after the braiding. Hence, detecting this energy shift reveals the non-Abelian statistics corre-

sponding to the Ising anyons.

We would like to thank Nick Read, Matthias Troyer and Zhenghan Wang for inspiring conversations. This work is supported by EPSRC, the Finnish Academy of Science, the EU Networks EMALI and SCALA and the Royal Society.

-
- [1] M.H. Freedman, A.Y. Kitaev, M.J. Larsen, and Z. Wang, *Bull. Amer. Math. Soc.* **40**, 31 (2004); G.K. Brennen and J.K. Pachos, *Proc. R. Soc. A* **10**, 1098 (2007); C. Nayak, S.H. Simon, A. Stern, M. Freedman, S. Das Sarma, *Rev. Mod. Phys.* **80**, 3 (2008).
 - [2] G. Moore and N. Read, *Nucl. Phys. B* **360**, 362 (1991); N. Read and D. Green, *Phys. Rev. B* **61**, 10267 (2000); N. Read and E. Rezayi, *Phys. Rev. B* **54**, 16864 (1996); N. Cooper, *Phys. Rev. Lett.* **92**, 220405 (2004).
 - [3] D. Vollhardt and P. Wölfle, *The Superfluid Phases of Helium 3* (Taylor & Francis, 1990); V. Gurarie and L. Radzihovsky, *Phys. Rev. B* **75**, 212509 (2007); D.A. Ivanov, *Phys. Rev. Lett.* **86**, 268 (2001); A. Stern, F. von Oppen and E. Mariani, *Phys. Rev. B* **70**, 205338 (2004); M. Stone and S.-B. Chung, *Phys. Rev. B* **73**, 014505 (2003).
 - [4] B. Douçot, L.B. Ioffe, and J. Vidal, *Phys. Rev. B* **69**, 214501 (2004); M. Levin and X.-G. Wen, *Phys. Rev. B* **71**, 045110 (2005); P. Fendley, *Ann. Phys.* **323**, 3113 (2007); J.R. Wootton, V. Lahtinen, Z. Wang and J.K. Pachos, *Phys. Rev. B* **78**, 161102(R) (2008); A.Y. Kitaev, *Ann. Phys.* **303**, 3 (2003).
 - [5] M.H. Freedman, C. Nayak and K. Shtengel, *Phys. Rev. Lett.* **94**, 066401 (2005).
 - [6] A.Y. Kitaev, *Ann. Phys.* **321**, 2 (2006).
 - [7] H. Yao and S.A. Kivelson, *Phys. Rev. Lett.* **99**, 247203 (2007).
 - [8] D. Arovas, J.R. Schrieffer and F. Wilczek, *Phys. Rev. Lett.* **53**, 722 (1984).
 - [9] Y. Tserkovnyak and S.H. Simon, *Phys. Rev. Lett.* **90**, 016802 (2003); S.-B. Chung and M. Stone, *J. Phys. A* **40**, 4923 (2007); C. Nayak and F. Wilczek, *Nucl. Phys. B* **479**, 529 (1996); V. Gurarie and C. Nayak, *Nucl. Phys. B* **506**, 685 (1997).
 - [10] N. Read, arXiv:0805.2507 (2008).
 - [11] V. Lahtinen, G. Kells, A. Carollo, T. Stitt, J. Vala and J.K. Pachos, *Ann. Phys.* **323**, 9 (2008).
 - [12] J. K. Pachos, *Ann. Phys.* **322**, 1254 (2007); G. Kells, A.T. Bolukbasi, V. Lahtinen, J.K. Slingerland, J.K. Pachos, J. Vala, *Phys. Rev. Lett.* **101**, 24 (2008)
 - [13] A. Micheli, G. K. Brennen, and P. Zoller, *Nature Physics* **2**, 341 (2005); L.M. Duan, E. Demler, and M.D. Lukin, *Phys. Rev. Lett.* **91**, 090402 (2003).
 - [14] J.K. Pachos and P. Zanardi, *Int. J. Mod. Phys. B* **15**, 1257 (2001).
 - [15] The states (6) are not symmetrized under gauge transformations (3). Nevertheless, their holonomy coincides with the holonomy of symmetrized states when C is a loop also in the space of gauge field configurations. This is due to the orthogonality of states belonging to different sectors of u .
 - [16] The holonomy (11) is only given up to a gauge transformation $g : \Gamma_C \rightarrow g\Gamma_C g^\dagger$ [10]. Before $s(U, V)$ can be evaluated, the gauge g must be fixed. Due to the finite size of

the system the two ground states are never perfectly degenerate (see Fig. 2), implying $g = \text{diag}(e^{i\phi_1}, e^{i\phi_2})$. This can be easily taken into account.

[17] Here $|U|$ denotes a matrix U with its elements replaced by their absolute values.